Rock Mech Rock Eng
DOI 10.1007/s00603-013-0428-1

ORIGINAL PAPER

An Approach for Modeling Rock Discontinuous Mechanical Behavior Under Multiphase Fluid Flow Conditions

Peng-Zhi Pan · Jonny Rutqvist · Xia-Ting Feng · Fei Yan

Received: 10 December 2012 / Accepted: 20 April 2013

Abstract In this paper, the two computer codes TOUGH2 and RDCA (for "rock discontinuous cellular automaton") are integrated for coupled hydromechanical analysis of multiphase fluid flow and discontinuous mechanical behavior in heterogeneous rock. TOUGH2 is a well-established code for geohydrological analysis involving multiphase, multicomponent fluid flow and heat transport; RDCA is a numerical model developed for simulating the nonlinear and discontinuous geomechanical behavior of rock. The RDCA incorporates the discontinuity of a fracture independently of the mesh, such that the fracture can be arbitrarily located within an element, while the fluid pressure calculated by TOUGH2 can be conveniently applied to fracture surfaces. We verify and demonstrate the coupled TOUGH–RDCA simulator by modeling a number of simulation examples related to coupled multiphase flow and geomechanical processes associated with the deep geological storage of carbon dioxide—including modeling of ground surface uplift, stress-dependent permeability, and the coupled multiphase flow and geomechanical behavior of fractures intersecting the caprock.

Keywords Rock discontinuous cellular automaton · TOUGH2 · CO_2 injection · Discontinuity · Multiphase flow

P.-Z. Pan (✉) · X.-T. Feng · F. Yan
State Key Laboratory of Geomechanics and Geotechnical Engineering, Institute of Rock and Soil Mechanics, Chinese Academy of Sciences, Wuhan 430071, China
e-mail: pzpan@whrsm.ac.cn

P.-Z. Pan · J. Rutqvist
Lawrence Berkeley National Laboratory, MS 90-1116, Berkeley, CA 94720, USA

1 Introduction

Coupled thermal-hydro-mechanical (THM) processes, which occur in a number of geoscientific fields and geoengineering applications, can be particularly strong and complex within fractured rock (Tsang 1999; Rutqvist et al. 2001; Neuzil 2003; Rutqvist and Stephansson 2003; Rutqvist 2012; Rutqvist and Tsang 2012). The analysis of such complex rock-mass behavior requires computer simulators with the capability to model coupled THM processes in heterogeneous and discontinuous geological media.

A growing number of coupled THM models for geological media have been developed in the last few decades. Among those, several simulators based on Biot's theory of consolidation, such as THAMES (Ohnishi et al. 1996), MOTIF (Guvanasen and Chan 1995), FRACON (Nguyen 1996) and ROCMAS (Noorishad et al. 1984), were developed and applied mostly to geological nuclear waste disposal. Other simulators [FEMH (Bower and Zyvoloski 1997), OpenGeoSys (Wang and Kolditz 2007), FRACTure (Kohl and Hopkirk 1995), GEOCRACK (Swenson et al. 1997)] were originally applied to the field of hot-dry-rock geothermal energy, although they have also been applied to other types of coupled problems. Some commercial codes [e.g., ABAQUS (Börgesson 1996), FLAC (Israelsson 1996a), and UDEC (Israelsson 1996b] have been applied in soil and rock mechanics. In the field of soil mechanics, COMPASS (Thomas and Sansom 1995) and CODE-BRIGHT (Olivella et al. 1994) were developed to simulate coupled two-phase (gas and liquid) fluid flow and thermo-mechanical responses in the partially saturated soil and isothermal multiphase flow of brine and gas in saline media. Most recently, codes capable of modeling coupled multiphase flow and geomechanics have been developed

Published online: 01 May 2013

for specialized applications such as geologic carbon sequestration, as well as for meeting a growing demand from the oil and gas industry to enhance production within unconventional oil and gas reservoirs (Ferronato et al. 2010; Rohmer and Seyedi 2010; Tran et al. 2010).

Many of the recent developments geared toward multiphase flow application are codes based on the linking of traditional multiphase flow reservoir simulators with geomechanical codes (Itasca Consulting Group 2000; Rutqvist and Tsang 2002; Rutqvist et al. 2002; Pruess and Spycher 2007). Rutqvist et al. (2002) developed and applied such an approach when linking the TOUGH2 multiphase flow simulator (Pruess and Spycher 2007) to the geomechanical simulator FLAC3D (Itasca Consulting Group I 2000). The resulting simulator TOUGH–FLAC has been successfully applied to a wide range of applications, including geologic carbon sequestration, nuclear waste disposal, underground compressed air energy storage, enhanced geothermal systems, and gas production from gas hydrates (Rutqvist 2011). However, because TOUGH–FLAC is based on a continuum approach, the ability to model nonlinear and discontinuous behavior in rock masses, including fracture propagation, is somewhat limited.

In this paper, we present an approach aimed toward effective modeling of coupled multiphase flow and geomechanical processes in strongly heterogeneous rock, including explicit modeling discontinuities such as fractures and faults. In this case, we utilized new developments related to the rock discontinuous cellular automaton (RDCA) modeling approach (Pan et al. 2012). Here we link RDCA with the TOUGH2 multiphase flow simulator to model coupled THM processes in strongly heterogeneous and discontinuous rock masses, including explicit modeling of multiphase fluid flow processes and their coupling to geomechanics. We first describe RDCA and TOUGH2 individually, then how they link together, and then follow with a number of numerical examples related to multiphase flow and geomechanical behavior associated with deep injection and geologic storage of CO_2 in deep sedimentary formations.

2 The RDCA and TOUGH2 and Their Linking

The RDCA code, which has been developed over the last few years, is based on the elasto-plastic cellular automaton (EPCA), which is an approach for modeling rock failure in heterogeneous rock developed at Institute of Rock and Soil Mechanics, Chinese Academy of Sciences, Wuhan, China (Feng et al. 2006; Pan et al. 2009a, b). The RDCA (Pan et al. 2012) includes the following features for modeling of fractures (or cracks) and their propagation: (1) a special displacement function to represent internal discontinuity; (2) a level set method to track the fracturing path; (3) partition of unity method to improve the integral precision of fracture-surface and fracture-tip representation; (4) a cellular automaton updating rule to calculate the mechanical state; (5) a mixed-mode fracture criterion to determine the fracturing behavior. This technique incorporates the discontinuity of the crack independently of the mesh, such that the crack can be arbitrarily located within an element. The method does not require any remeshing for crack growth, an aspect that greatly reduces the complexity and improves the efficiency in modeling rock-fracture geomechanical behavior. Currently, the RDCA is a 2-dimensional model. A nodal-based space discretization method (e.g., FEM) is used. The displacement vector is located at element (isoparametric element) vertices. A shape function is used to interpolate the displacement field within each element based on the displacement at element vertices. Unlike the continuum method, we introduce special shape functions, i.e., the Heaviside function (step function) to simulate the crack surface, and the asymptotic crack-tip displacement field function, to approximate a discontinuous displacement field. RDCA inherits all the features from EPCA (Feng et al. 2006; Pan et al. 2009a, b) and the elasto-plastic analysis (non-associated plastic flow law) can be considered. In the work presented in this paper, we limit the model description and analysis to the mechanical behavior of pre-existing fractures. (Note that fluid-driven fracture propagation will be the subject of future studies.)

TOUGH2 is a numerical simulator developed at the Lawrence Berkeley National Laboratory, Berkeley, California, for multidimensional fluid and heat flows of multiphase, multicomponent fluid mixtures in porous and fractured media (Pruess et al. 1999). The first version of this code was developed in the early 1980s, primarily for geothermal reservoir engineering, but it is now widely used by universities, government organizations, and private industry for applications to nuclear waste disposal, environmental remediation problems, energy production from geothermal sources, and oil and gas reservoirs—as well as gas hydrate deposits, geological carbon sequestration, and vadose zone hydrology. TOUGH2 uses space discretization by integral finite differences (IFD), for 1-D, 2-D, or 3-D regular or irregular grid geometries, and is applicable to single porosity or multi continua (fractured media). It uses fully implicit time weighting with simultaneous, iterative solutions of all mass and energy balances, whereas phase (dis-)appearance is handled by switching primary variables. Currently, TOUGH simulators are being continually updated, with new equation-of-state (EOS) modules being developed and refined process descriptions implemented into the TOUGH framework. Notably, a number of EOS property modules for mixtures of water, NaCl, and CO_2 have been recently developed and are already widely used

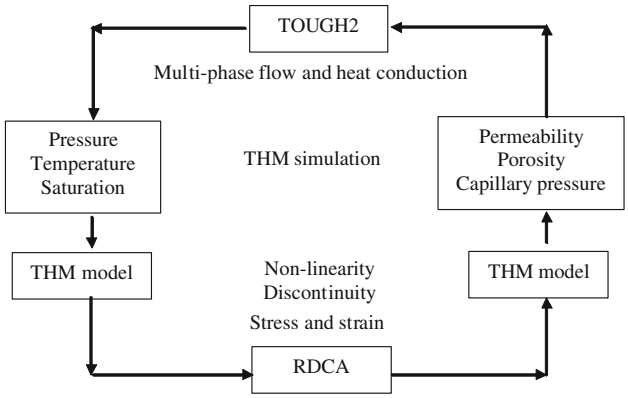

Fig. 1 Schematic of linking TOUGH2 and EPCA for coupled thermo-hydro-mechanical (THM) simulations

for the analysis of geologic carbon sequestration processes (Pruess and Spycher 2007).

Figure 1 shows the linking of TOUGH2 and RDCA codes related to THM processes modeling. The two codes are linked sequentially, following the approach of Rutqvist et al. (2011). Therefore, the linking of these two codes is a "double-way" approach. A TOUGH-to-RDCA link takes multiphase temperatures, pressures, and saturations from the TOUGH2 simulation and provides that information to RDCA. In RDCA, thermal expansion and effective stress are calculated, and then a failure analysis (plasticity or discontinuity) is conducted. Conversely, an RDCA-to-TOUGH link takes the mechanical variables (stress, plastic strain or fracture-opening displacement) from RDCA and updates the corresponding element porosity, permeability, and capillary pressure to be used by TOUGH2. To run a TOUGH–RDCA simulation, the numerical grids for the two codes must be developed with the same geometry and element numbering.

In linking TOUGH2 with RDCA, special attention is devoted to the modeling of discontinuities. As mentioned, in RDCA the fracture geometry (or other internal boundaries) and the numerical grid are independent of each other. By using a level set method, we divide the elements intersected by a fracture into several quadrilateral subelements along the fracture surface Γ_c, based on the *partition of unity* concept (Fig. 2). According to the distribution of the fluid field, each element in RDCA may have a certain magnitude of fluid pressure. For elements intersected by a crack, the fluid pressure is applied on the two opposing fracture surfaces, Γ_c^+ and Γ_c^-. Gaussian quadrature points are defined along each of the one-dimensional subelements to numerically integrate the terms on Γ_c (Fig. 3). Each Gaussian point coordinate on Γ_c is mapped on global coordinates, which are then mapped within the local coordinate system on the cell elements intersected by a fracture. The Gaussian quadrature is performed by a loop over one-dimensional elements. The nodal forces induced by fluid pressure on the fracture surface and fracture tip can be, respectively, calculated as

$$f_i^a = 2\int_{\Gamma_c} n \cdot N_i p \mathrm{d}\Gamma \tag{1}$$

$$f_i^{b\alpha} = 2\int_{\Gamma_c} n\sqrt{r} \cdot N_i p \mathrm{d}\Gamma \quad \alpha = 1,2,3,4 \tag{2}$$

where p is the fluid pressure applied on the fracture surfaces, n is a vector normal to the fracture surfaces, r is the radius for integration around the fracture tip, and N_i is a shape function.

In this study, we consider discontinuities such as fractures and faults that may undergo opening and shearing resulting from stick and slip. The contact behavior is described by the shear stiffnessK_s, the normal stiffness K_n, and the frictional coefficient μ. The stick mode, i.e., $t_n < 0$ and $t_s < |t_n|\mu$, depends on K_s and K_n at nodes inside each one-dimensional element by

$$t_s = K_s D_s,\ t_n = K_n D_n \tag{3}$$

where t_s and t_n are shear and normal tractions, respectively; and D_s and D_n are, respectively, the shear and normal displacement on the fracture surfaces.

If $t_n > 0$, the crack is open, corresponding to complete loss of contact between the two rough-walled fracture surfaces. In such a case, the shear and normal tractions vanish, i.e.,

$$t_s = 0, \quad t_n = 0 \tag{4}$$

If $t_n < 0$ and $|t_s| \geq |t_n|\mu$, a relative tangential slip occurs.

When linking TOUGH2 with RDCA, we apply the fluid pressure from TOUGH2 to RDCA cells as well as to the internal fracture surfaces. Figure 4 shows that in the case of fluid injection, the fluid pressure applied on fracture surfaces may be non-uniform, resulting in non-uniform nodal force distribution. According to the magnitude of fluid pressure on each element, the equivalent nodal force can be calculated based on the effective stress theory. For normal elements, i.e., without a fracture, the equivalent nodal forces can be calculated by (for 2D problem)

$$\{f\}^e = \int_{\Omega^e} [B]^T \{p, p, 0\}^T d\Omega \tag{5}$$

where p is the fluid pressure and B is the strain–displacement matrix.

For elements that include a fracture with two opposing fracture surfaces and fracture tips, the equivalent nodal force includes two components. One is from the fluid pressure applied on the fracture surfaces, as calculated by Eqs. (1) and (2). The other is from the subelements, which

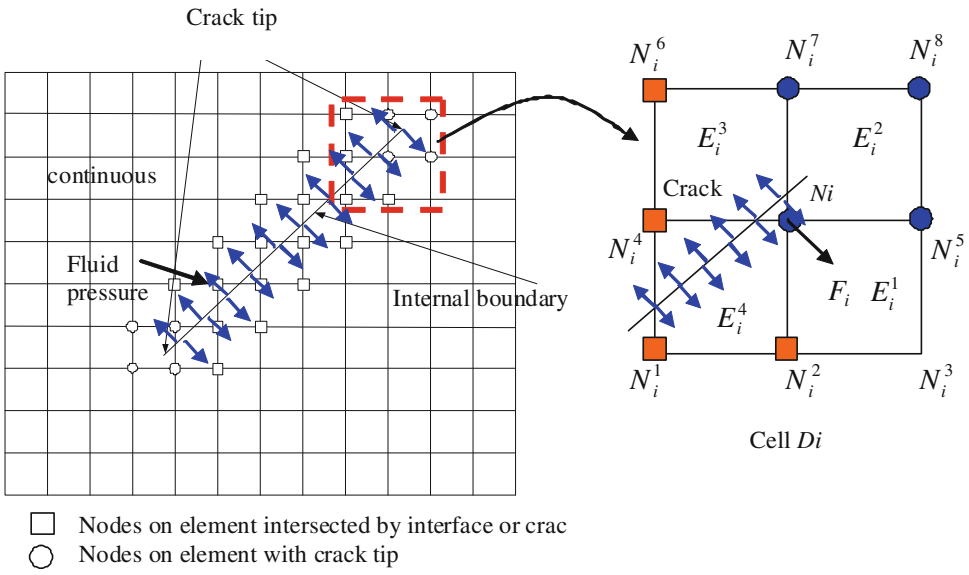

Fig. 2 Crack representation in the discontinuous cellular automaton modeling approach

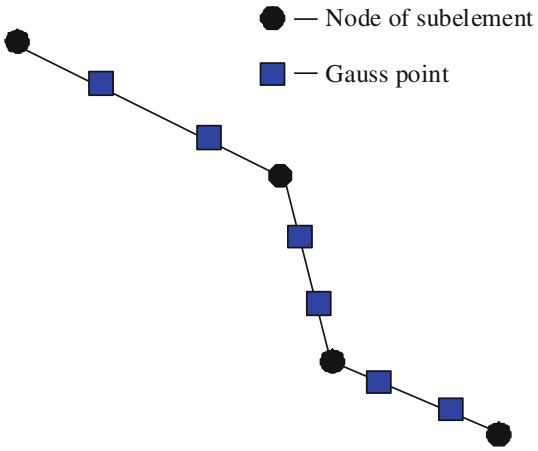

Fig. 3 Gauss quadrature points distributed along the crack

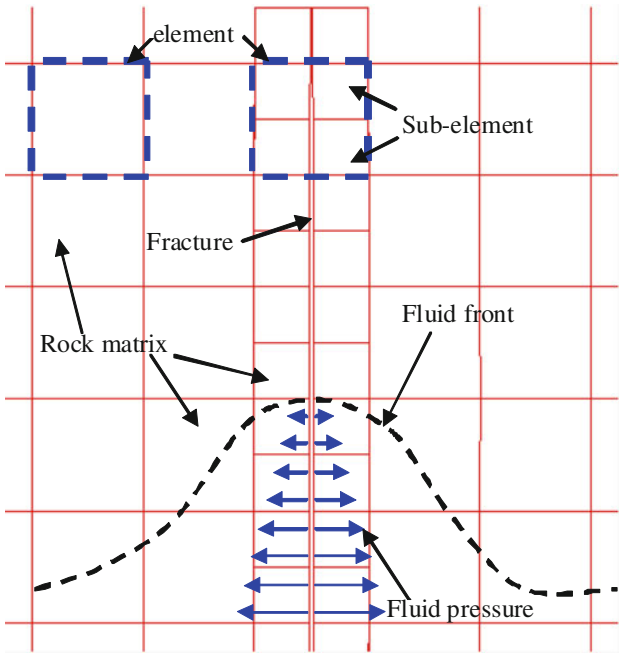

Fig. 4 The mechanical state of rock mass induced by fluid flow

are regarded as rock matrix. Therefore, the contribution of subelements to element equivalent nodal force can be calculated by Eq. (3), in which the matrix B is different from the normal element and the nodal force belongs to additional degrees of freedom.

In a linked TOUGH2 and RDCA simulation, the two codes are executed sequentially, following the approach used in Rutqvist et al. (2002) for coupling TOUGH2 and FLAC3D. The user first prepares the numerical grid and input parameters for each of the simulators using mutually consistent grids. The input parameters for the TOUGH simulation include grain density, porosity, permeability, thermal conductivity, specific heat, relative permeability and water retention curves, as well as hydraulic and thermal boundary conditions (e.g., fixed fluid pressure and temperature). Typical input parameters for the RDCA simulation include bulk density, elastic parameters (Young's modulus, Poisson's ratio), fracture mechanical parameters (e.g., normal stiffness, shear stiffness, coefficient of friction, and fracture toughness), as well as mechanical boundary conditions (e.g., fixed displacement or stress).

The simulations might first be conducted in both of the codes to establish initial conditions and perhaps to make a test simulation without considering the coupling of fluid flow and geomechanical processes. Then, in the full TOUGH–RDCA simulation, an external routine would contain appropriate coupling functions for linking the two codes. For example, porosity, permeability, and capillary pressure functions are dependent on certain mechanical

variables, such as mean stress, volumetric strain, or fracture aperture.

3 Numerical Example Related to Geologic CO_2 Storage

We present a number of numerical examples related to the geologic storage of CO_2. The simulations are focused on demonstrating how a TOUGH–RDCA simulation could address some key geomechanical issues related to CO_2 storage in deep sedimentary formations, including caprock sealing performance and the effects on fractures and faults intersecting the caprock (Rutqvist 2012). First, we conduct simulations related to CO_2 injection into a reservoir–caprock system, according to a simulation example developed and solved in Rutqvist and Tsang (2002). Rutqvist and Tsang (2002) applied TOUGH–FLAC to study caprock hydromechanical changes associated with CO_2-injection into a brine formation, and by comparison with those results, we verify the implementation of the basic TOUGH–RDCA coupling for cases without discontinuities. We then expand the analysis to include discontinuities in the caprock, applying this method for multiphase fluid flow and geomechanical processes using the TOUGH–RDCA simulator.

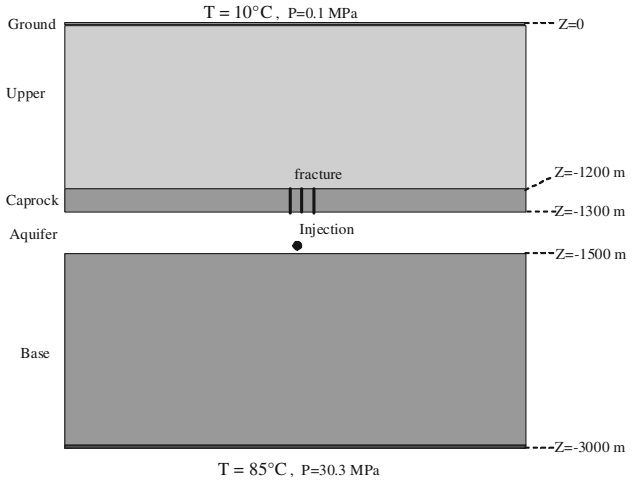

Fig. 5 Description of model simulation related to injection and geologic storage of CO_2 in deep sedimentary formations

3.1 Problem Description

Figure 5 presents the basic model geometry for cases with and without discontinuities. In all simulation cases, CO_2 was injected into a 300-m-thick injection zone located at 1,200–1,500 m depth. The overburden consists of a 1,000-m-thick upper layer and a 200-m-thick caprock located just above the injection zone. Over a 10-year period, CO_2 was injected at a constant flow rate of 0.05 kg/s per meter normal to the model plane (Rutqvist and Tsang 2002). This flow rate is equivalent to 1.6 Mt/year if the injection were conducted along a 1,000-m-thick section of the reservoir normal to the model plane (for example, representing the injection rate for a 1 km long horizontal well). We may also relate this to real injection rates at the In Salah CO_2 storage project, where injection rates have been 0.5–1.0 million tons per year, distributed over three horizontal injection wells, each 1–1.5 km long (Rutqvist et al. 2010).

For unfractured porous rock or for the rock matrix between fractures, the constitutive relationships of an isotropic linear poroelastic medium can be expressed in terms of the effective stress σ'_{ij} (positive for tension), strain ε_{ij}, and temperature change ΔT as (Pan et al. 2009a)

$$\sigma'_{ij} = 2G\left(\varepsilon_{ij} + \delta_{ij}\frac{v}{1-2v}\varepsilon_{kk}\right) - K'\alpha\Delta T\delta_{ij} \tag{6}$$

where $\sigma'_{ij} = \sigma_{ij} + \xi\bar{p}\delta_{ij}$ and σ_{ij} is the total stress (positive for tension), δ_{ij} is the Kronecker's delta, and $\xi(\leq 1)$ is a

Table 1 Rock matrix material properties

Property	Upper	Cap	Aquifer	Basement
Young's modulus, E (GPa)	5	5	5	5
Poisson's ratio, v (−)	0.25	0.25	0.25	0.25
Biot's parameter, a (−)	1	1	1	1
Saturated rock density, ρ_s (kg/m^3)	2,260	2,260	2,260	2,260
Zero stress porosity, ϕ_0 (−)	0.1	0.01	0.1	0.01
Residual porosity, ϕ_r (−)	0.09	0.009	0.09	0.009
Zero stress permeability, k_0 (m^2)	le−15	le−17	le−13	le−17
Corey's irreducible gas saturation, S_{rg} (−)	0.05	0.05	0.05	0.05
Corey's irreducible liquid saturation, S_{rl} (−)	0.3	0.3	0.3	0.3
van Genuchten's air-entry pressure, P_0 (kPa) (at zero stress)	196	3,100	19.6	3,100
van Genuchten's exponent, m	0.457	0.457	0.457	0.457
Thermal expansion coefficient, γ (l/ °C)	7e−6	7e−6	7e−6	7e−6

coefficient that depends on the compressibility of the constituents. Here, $\xi = 1$ is assumed. $\bar{p}$ is an average pore pressure defined as:

$$\bar{p} = S_l p_l + (1 - S_l) p_g. \tag{7}$$

For rock fractures, the fluid pressure is applied on and normal to the two opposing fracture surfaces. The effective stress normal across the fracture is expressed as:

$$\sigma_n' = \sigma_n + \xi \bar{p}. \tag{8}$$

For the rock matrix, isotropic, hydromechanical rock properties are represented by porosity–mean stress and permeability–porosity relationships. The porosity, ϕ, is related to the mean effective stress as (Rutqvist and Tsang 2002)

$$\phi = (\phi_0 - \phi_r) \exp\left(5 \times 10^{-8} \times \sigma_M'\right) + \phi_r \tag{9}$$

where ϕ_0 is porosity at zero stress, ϕ_r is residual porosity at high stress, and the mean effective stress (in Pa) is defined from the stress components as:

$$\sigma_M' = \frac{1}{3}\left(\sigma_x' + \sigma_y' + \sigma_z'\right). \tag{10}$$

The permeability is correlated to the porosity according to the following exponential function

$$k = k_0 \exp[22.2(\phi/\phi_0 - 1)] \tag{11}$$

where k_0 is the zero stress permeability. Equations (9) and (11) were parameterized by respective 5×10^{-8} Pa^{-1} and 22.2 in Rutqvist and Tsang (2002) by fitting against laboratory data on sandstone.

The permeability of the continuum element intersected by a fracture is calculated as

$$k = k_m + k_f \tag{12}$$

where k_m is the rock matrix permeability and k_f is the fracture permeability. The fracture permeability is calculated by the cubic relation between aperture and fracture flow according to the following approximate equation:

$$k_f = \frac{h^3}{12b} \tag{13}$$

where b is estimated as the mean size of the element taken as the square root of the element area and h is hydraulic conducting aperture. Equations (12) and (13) provide a simplification related to the estimation of b, but will be

Table 2 Fracture properties

Property	Normal stiffness, Kn (Pa/m)	Shear stiffness, Ks (Pa/m)	Friction coefficient
Value	5e11	1e11	0.3

Table 3 Initial conditions in caprock and aquifer before injection

Parameter	Caprock	Aquifer
Temperature, T (°C)	40–42.5	42.5–47.5
Pressure, P (MPa)	12.1–13.1	13.1–15.1
Mean stress, σ_M'(MPa)	26.6–28.8	28.8–33.2
Porosity, ϕ (−)	0.0094	0.094
Permeability, k_0 (m^2)	0.3e−17	0.3e−13
Van Genuchten's air-entry pressure, P_0 (kPa)	5,800	36.8

Values are given as a range because they vary with depth in each formation

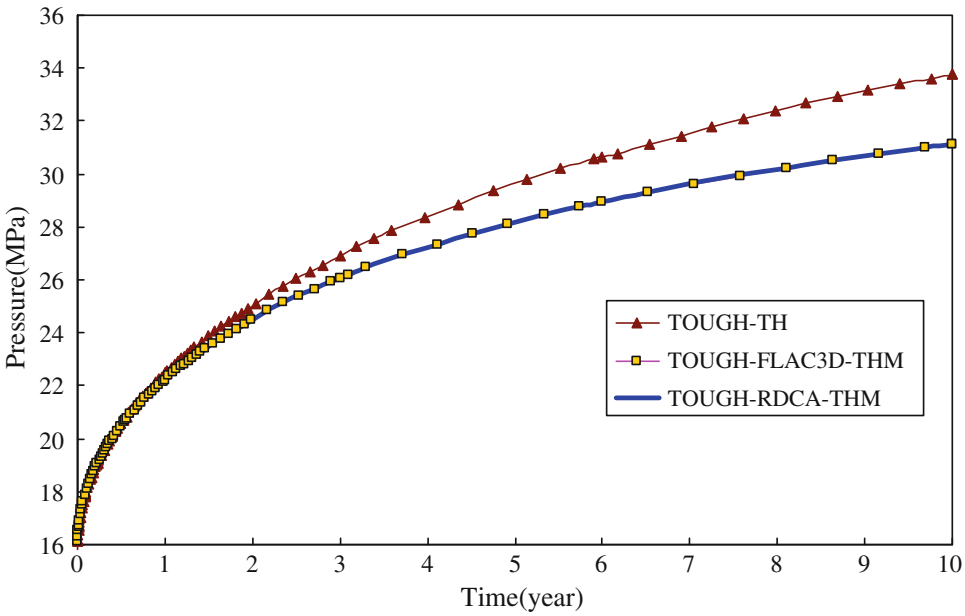

Fig. 6 Injection pressure as a function of time with and without considering hydro-mechanical coupling effects—comparisons between different simulators

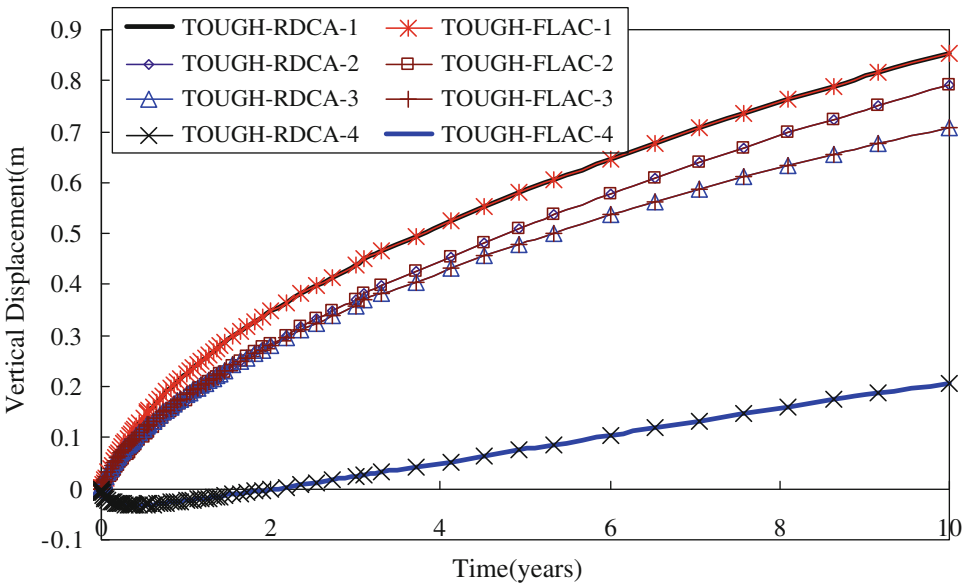

Fig. 7 Vertical displacements during 10 years of CO_2 injection on four points [i.e., (1) top of well at ground surface, (2) top of caprock, (3) top of injection zone and (4) bottom of injection zone] using different

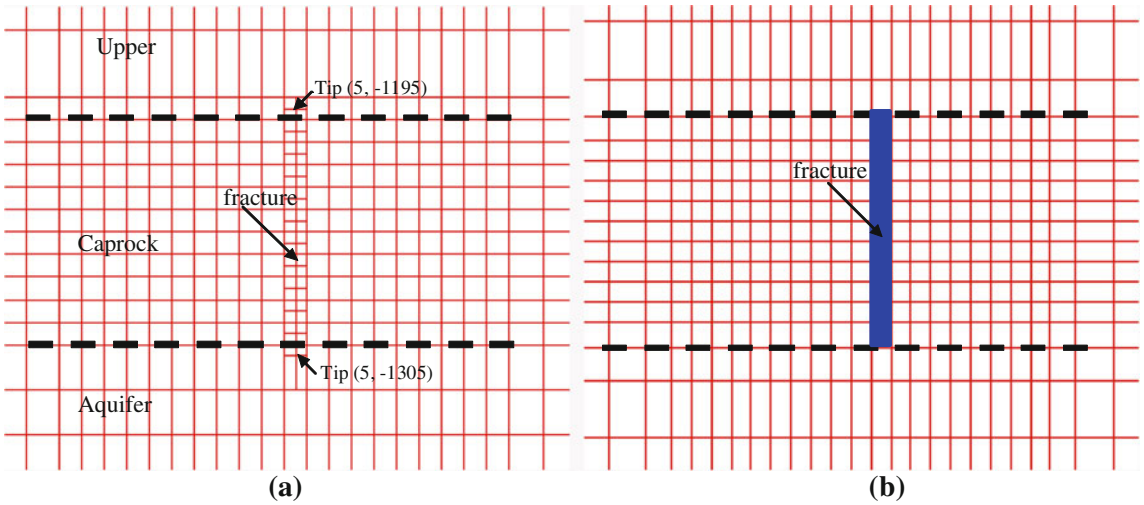

Fig. 8 Grids used in **a** RDCA and **b** TOUGH2

reasonably accurate as the resulting permeability is strongly dependent on *h* through its cubic dependency.

Tables 1, 2, 3 present rock matrix properties, rock fracture parameters, and initial conditions used in the modeling. The fluid-property module ECO2N (Pruess and Spycher 2007) was employed for modeling the thermodynamic and thermophysical properties of water–NaCl–CO_2 mixtures. The relative permeability of gas and liquid phases is calculated from Corey's function (Corey 1954), while capillary pressure is governed by the van Genuchten function (1980). Detailed model description and parameters can be found in Rutqvist and Tsang (2002).

3.2 Homogeneous (Intact) Caprock

The application of TOUGH–RDCA starts with a case of a homogeneous (intact) caprock without fractures. As mentioned, this case was simulated by Rutqvist and Tsang (2002) using the TOUGH–FLAC simulator; the purpose of our simulation of the same case is a code-to-code verification of the TOUGH–RDCA coupling algorithms. Figures 6 and 7 present a comparison between simulation results using the two different simulators. The good agreement indicates that TOUGH–RDCA works very well.

3.3 Effects of Discontinuities in the Caprock

As mentioned, the RDCA incorporates rock discontinuities—such as minor cracks, fractures and faults—independently of the mesh, such that any discontinuity can be arbitrarily located within an element. The method does not require any remeshing for discontinuity growth (fracture propagation), greatly simplifying the modeling procedure and the combining of RDCA with TOUGH2. In a

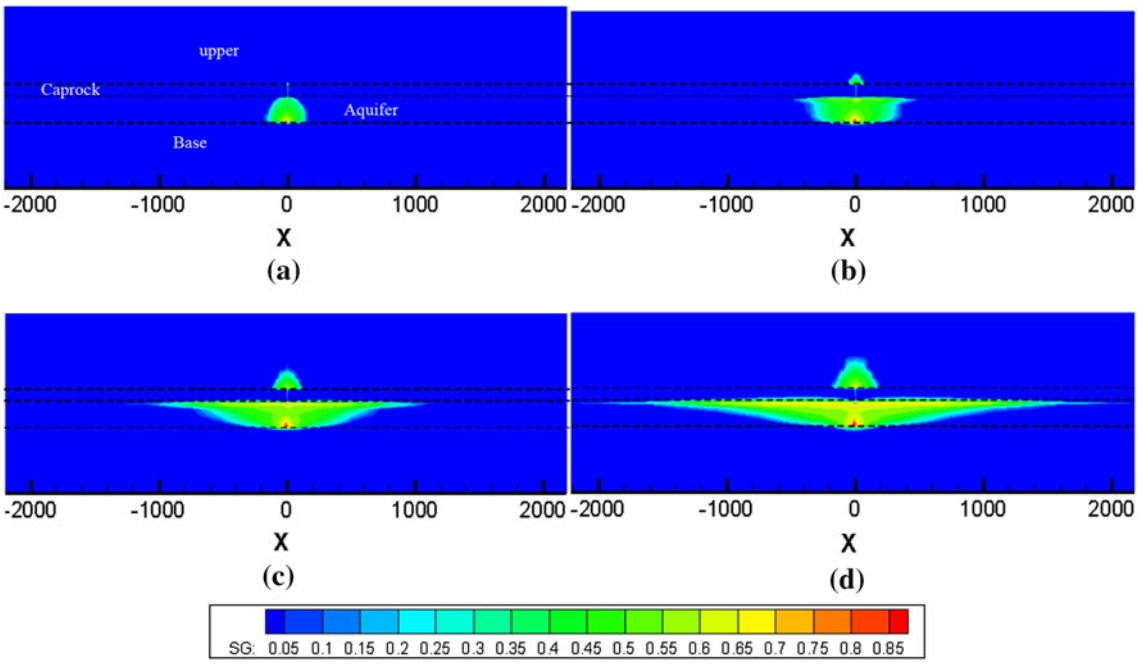

Fig. 9 CO_2 saturation during active CO_2 injection at **a** 1 year, **b** 3 years, **c** 6 years and **d** 10 years

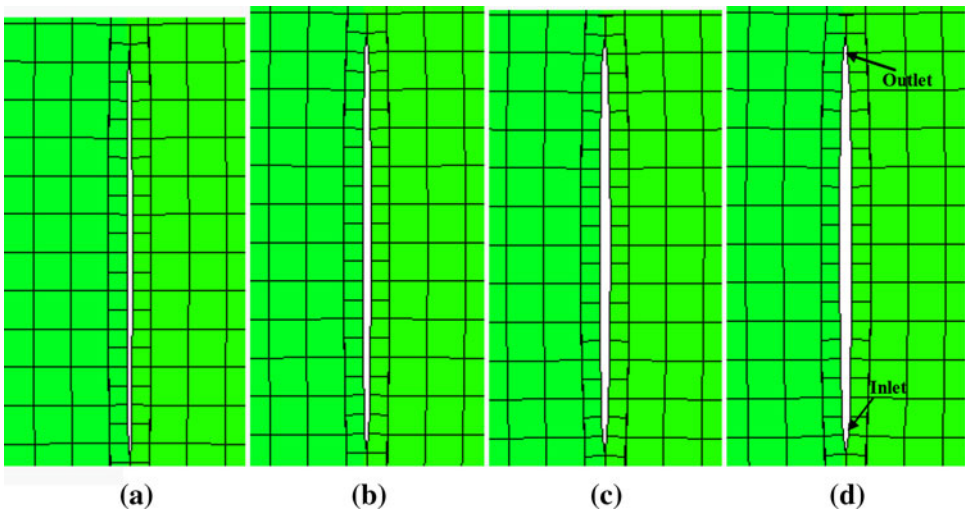

Fig. 10 The fracture-surface deformation (enlarge 1,000 times) during the injection of CO_2. **a** 1 year, **b** 3 year, **c** 6 year and **d** 10 year

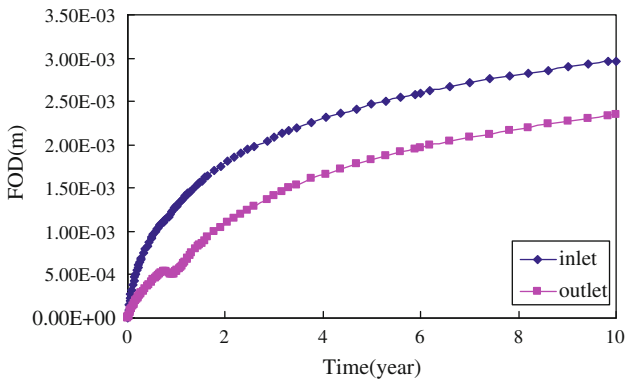

Fig. 11 Fracture normal displacement evolution at inlet and outlet

TOUGH–RDCA simulation, the discontinuous geometry is updated in the RDCA through the level set method, and the updated geometry is transferred to TOUGH after each time step. Several examples are presented below to demonstrate this capability.

3.3.1 Single Fracture Behavior

As a first simulation example, we introduce a discontinuity representing a vertical fracture intersecting the caprock and study its influence on caprock HM behavior. In RDCA, the discontinuity representing the fracture is regarded as an internal boundary, in which the discontinuous boundary coincides with the edge of subelements; whereas in

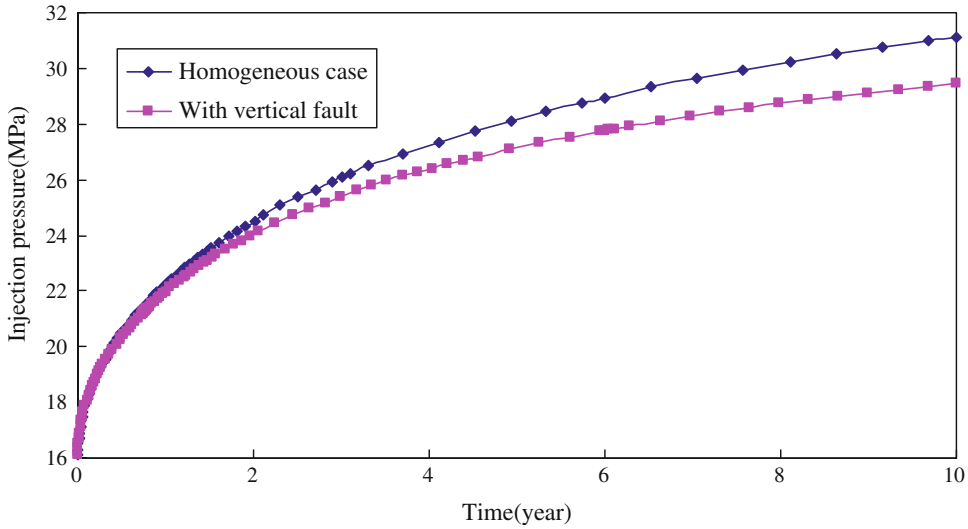

Fig. 12 Injection pressure as a function of time with and without considering fracture in caprock

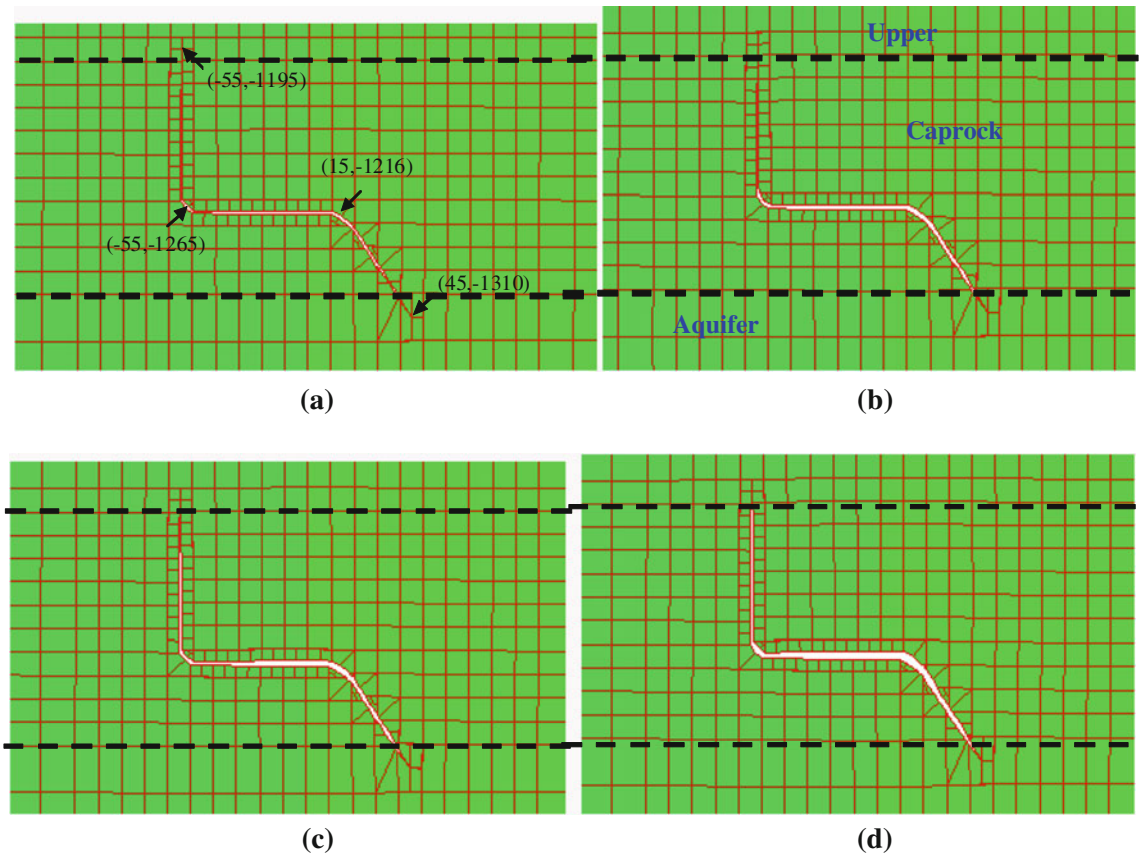

Fig. 13 The fracture behavior during injection of CO_2 (enlarged 1,000 times). **a** 12 months, **b** 15 months, **c** 18 months and **d** 36 months

TOUGH2, the hydraulic behavior of the fracture is modeled using an equivalent porous medium approach (Fig. 8). In this model simulation, TOUGH2 elements containing the fracture have initially the same permeability as the caprock matrix rock, meaning that the fracture is completely sealed. During the subsequent active fluid injection, the fracture opens as a result of increased internal fluid pressure and becomes more permeable than the surrounding caprock.

Figure 9 shows the evolution of the CO_2 plume as a result of the constant-rate injection. Already after 1 year of injection, the CO_2 has penetrated into the fracture, but not yet up into the overlying aquifer. As the permeability of the fracture is much higher than the surrounding caprock, the

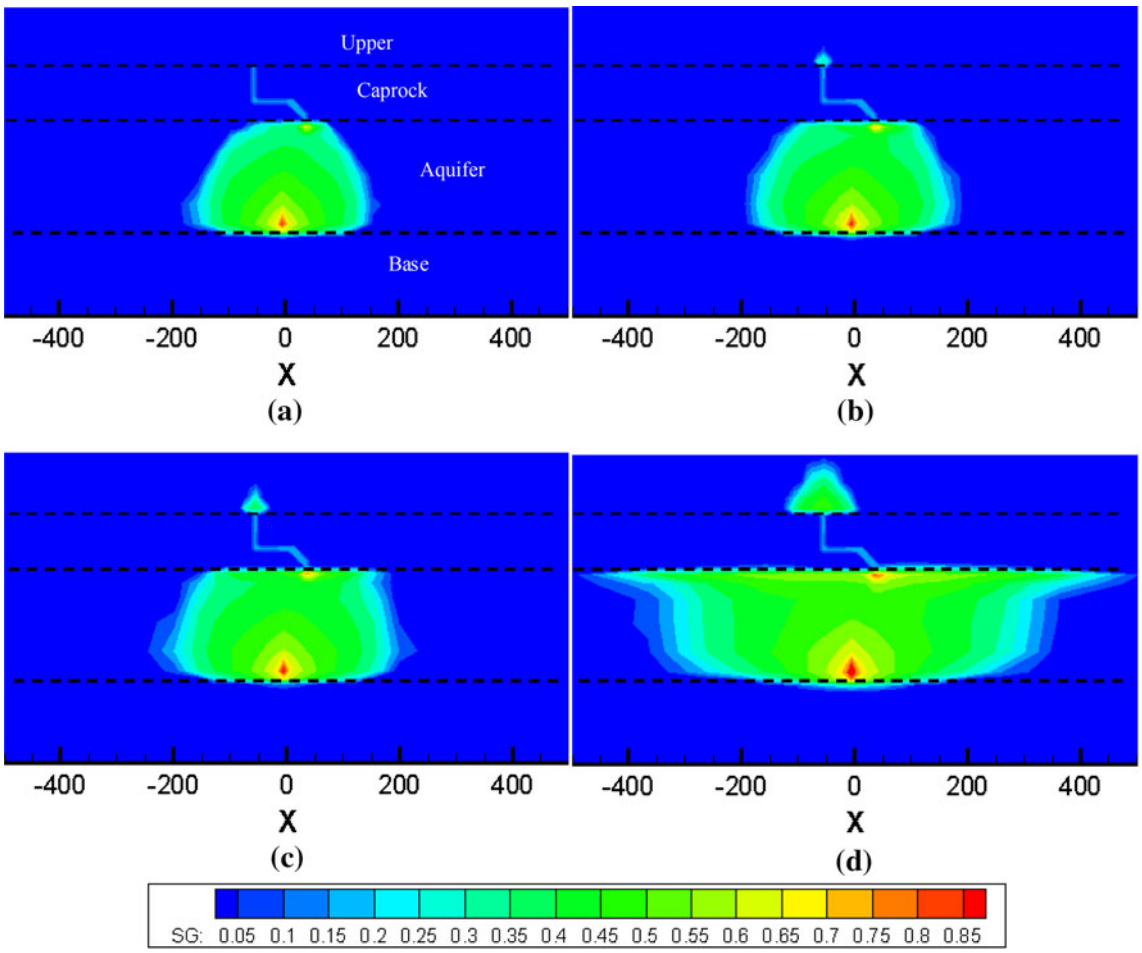

Fig. 14 CO_2 saturation evolution process during injection. **a** 12 months, **b** 15 months, **c** 18 months and **d** 36 months

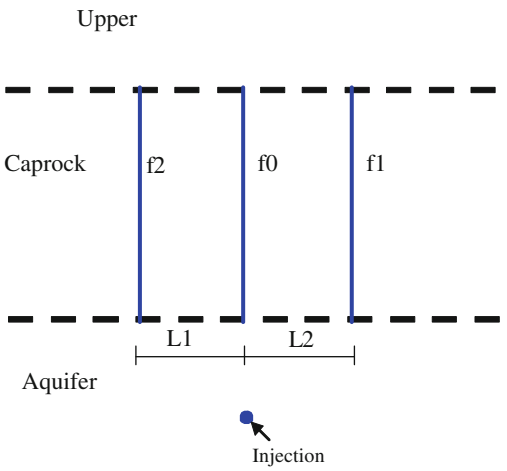

Cases	L1 (m)	L2 (m)
0	0	0
1	40	40
2	70	70
3	90	90

Fig. 15 Different modeling cases with different fracture layouts (*f0*, *f1* and *f2* are fractures in caprock)

CO_2 migrates very quickly along the fracture, and a significant amount of CO_2 infiltrates the caprock (Fig. 9). After 10 years of injection, the CO_2 plume has penetrated into the upper aquifer and spread laterally (as well as upwards) about 200 m by buoyancy.

Figures 10 and 11 show the evolution of fracture-surface deformation. Figure 10 shows how the fracture opens, with the maximum opening at the center distance between the two crack tips, located just above and below the caprock. Figure 11 shows the evolution of fracture normal displacement at the inlet (at the bottom of the caprock) and outlet (at the top of the caprock). The fracture opens more at the inlet, because of the higher pressure changes compared to that at the outlet. The fracture-opening

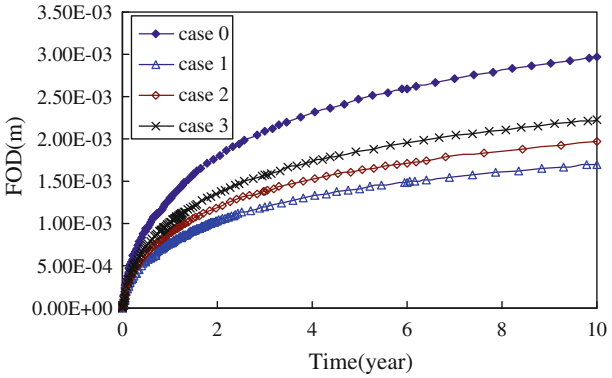

Fig. 16 The fracture-opening displacements of fracture f0 at inlet for different cases

displacement (FOD) at inlet rises to 2.97 mm after 10 years of injection. As a result of the existence of the vertical fault (or fracture) within the rock mass, some of the reservoir pressure can be released. As a result, after 10 years of injection, the injection pressure decreases about 1.14 MPa compared with the result for the homogeneous case (Fig. 12).

Since the geometry of the discontinuities are independent of the numerical mesh, an arbitrary fracture geometry can be conveniently simulated. Figures 13 and 14 result from the case of a zigzag caprock fracture geometry, through simply updating the discontinuity geometry in RDCA. This could represent the formation of fracture openings along three intersecting fractures (one inclined, one horizontal, and one vertical) in a fracture network that might exist in the caprock. Here, we assumed the arbitrary geometry to demonstrate the versatility of the TOUGH–RDCA code: it conveniently discretizes fractures of various orientations. Similarly to the vertical fracture case, the fracture opens gradually along with the increasing reservoir pressure, and CO_2 breaks through and migrates upwards by buoyancy along with the pressure gradient.

3.3.2 The Interaction Between Multiple Fractures

The previous section presents the results from coupled multiphase flow and geomechanical behavior when considering one fracture in the caprock. In another scenario, we studied the effects and interactions of multiple fractures (or faults) (Fig. 15). Following the previous modeling case (i.e., case 0 in Fig. 15), two other fractures (f1 and f2) are located at both sides of the central fracture (f0). The CO_2 is injected at the point (the same place as in the previous case,

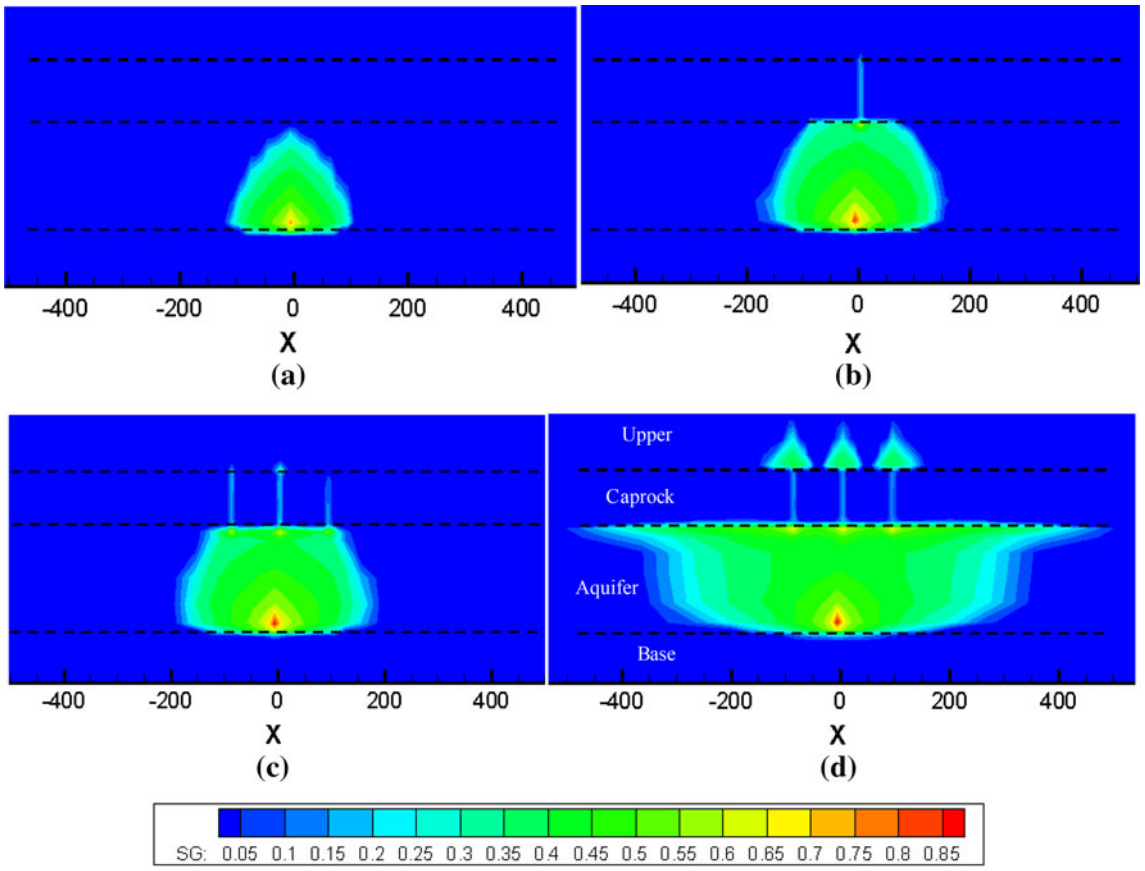

Fig. 17 CO_2 saturation evolution for case 3. **a** 6 months, **b** 9 months, **c** 1 year and **d** 3 years

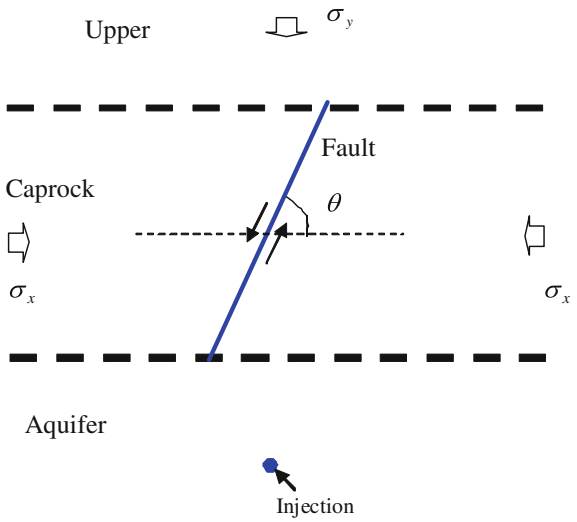

Cases	θ
1	75
2	60
3	45

Fig. 18 Schematic of one fracture (or fault) with different inclinations in the caprock

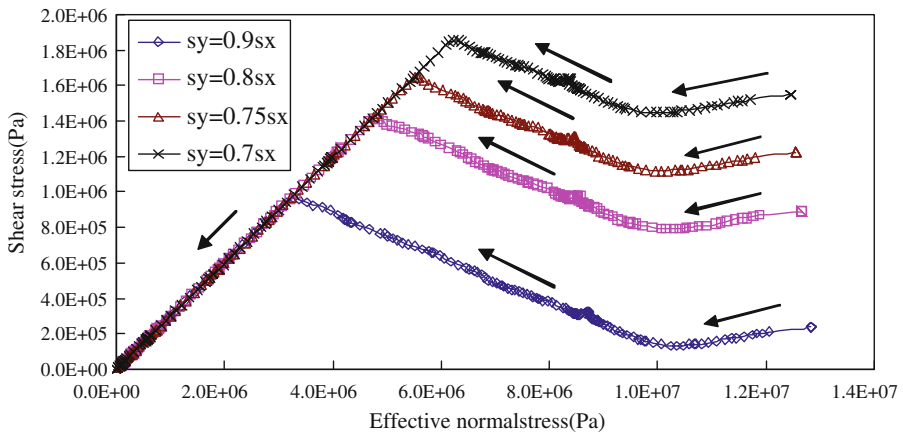

(a)

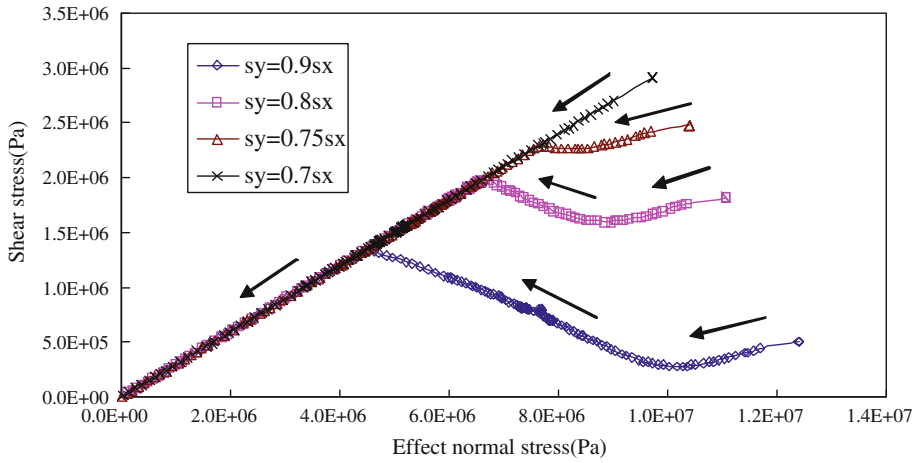

(b)

Fig. 19 The relation between effective normal stress and shear stress of fracture with different inclinations, considering different ratios between vertical and *horizontal* stresses. **a** 75° and **b** 45°. (*Arrows* in the figure indicate the stress path direction)

case 0) right below the central fault (f0) in the aquifer. By considering different distances between f0 and the other faults (f1 and f2), we can track the injection fluid-pressure evolution, CO_2 transport, and fracture-opening displacements. We found in this simulation that with the additional fractures, the injection pressure after 10 years of injection is on average 0.47 MPa lower than the case (case 0) with only one vertical fracture.

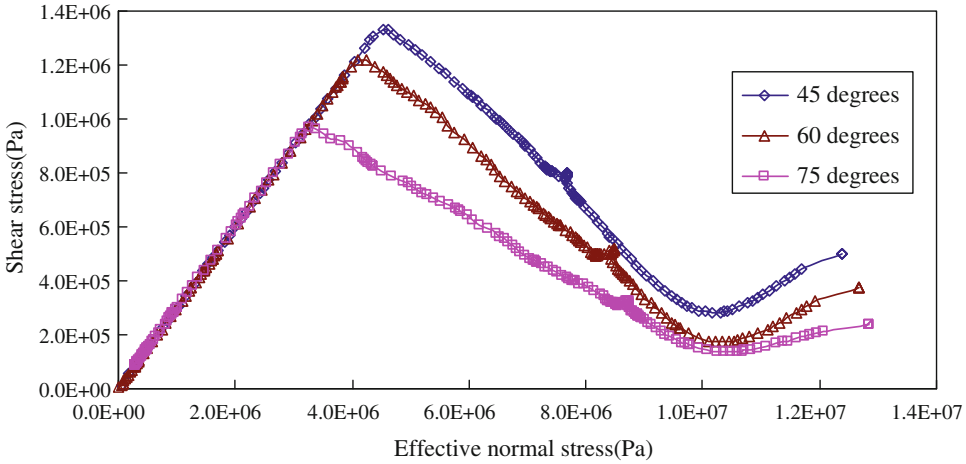

Fig. 20 The relation between effective normal stress and shear stress of fracture with different inclinations ($\sigma_y/\sigma_x = 0.9$)

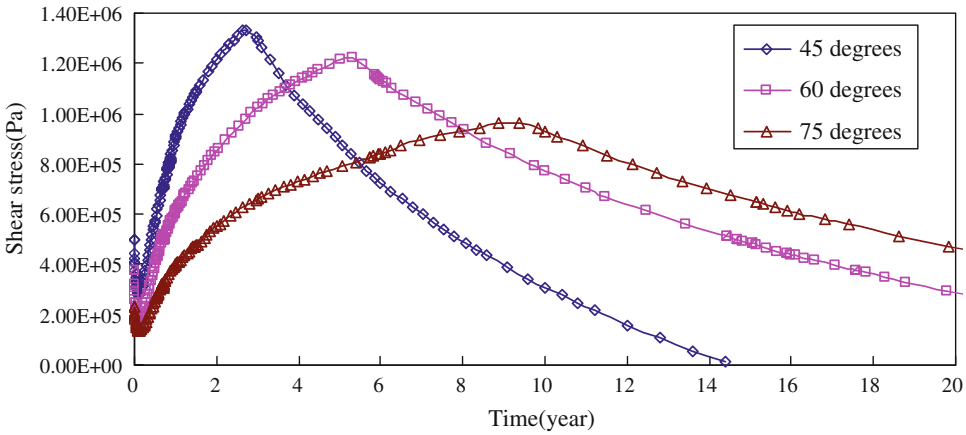

Fig. 21 The evolution of shear stress on fracture with different inclinations during CO_2 injection ($\sigma_y/\sigma_x = 0.9$)

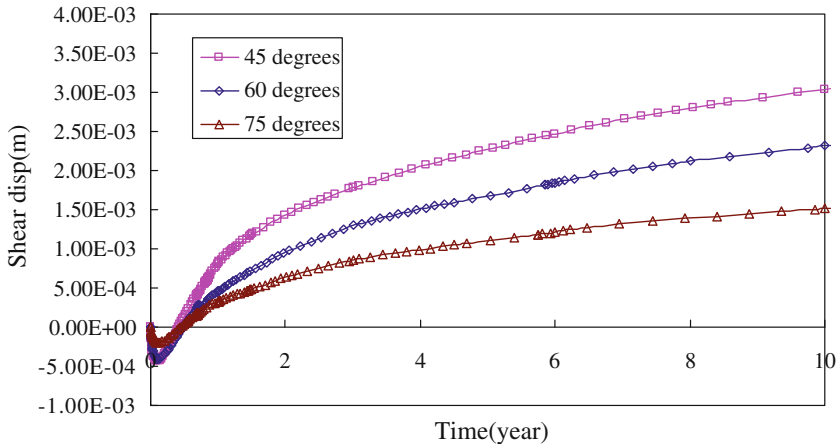

Fig. 22 Variation of shear displacement of fracture with different inclinations ($\sigma_y/\sigma_x = 0.9$)

The crack surface deformation over 10 years of injection is presented in Fig. 16. The existence of f1 and f2 and their opening restricts the opening of f0. This restriction weakens with the increase in distance (L1 and L2). After 9 months, the CO_2 migrates through the central fracture and quickly fills the fracture space. The other two fractures are filled with CO_2 after 1 year's injection. After 3 years, the CO_2 migrates through caprock from the three fractures and spreads within the upper layer (Fig. 17). Compared with case 0 (Fig. 9b), the amount and the spread range of the CO_2 from the central fracture are smaller in case 3 after 3 years of injection.

3.3.3 Inclined Fractures (Or Faults) Under Anisotropic Stress

In the above cases, we use an isotropic initial stress field, i.e., vertical stress and horizontal stress are the same. In

such a case, the shear stress on the fracture surface should theoretically be zero. Although the heterogeneous stress field induced by the presence of fractures will lead to small shear stresses on the fracture surface, the shear effect is not prominent. Therefore, in this section, we use an anisotropic initial stress field to study the effect of fractures (or faults) with different inclinations in the caprock. The purpose of this simulation case is to test and demonstrate TOUGH–RDCA's capability to simulate fracture shear or fault activation with fractures crossing the numerical grid at different angles.

Different inclinations (75°, 60°, 45°) and different stress ratios ($\sigma_y/\sigma_x = 0.9, 0.8, 0.75, 0.7$) are considered (Fig. 18). Other physical parameters are the same as in previous cases. In the modeling, the shear displacements, shear stress, and normal stress at the central point of the fracture surface are monitored. Figure 19 shows the relationship between effective normal stress and shear stress of fracture with inclination angles 75° and 45°. With the injection of CO_2, the increase in fluid pressure within the fracture leads to a decrease in effective normal stress. As a result, the shear stress first increases and then decreases when the slide condition is met ($t_n < 0$ and $|t_s| \geq |t_n|\mu$), as shown in Fig. 19. It can be seen that the smaller the stress ratio σ_y/σ_x, the earlier the fracture slides—especially for the 45° inclination, the fault begins sliding before the injection of CO_2 for the case of stress ratio$\sigma_y/\sigma_x = 0.7$. This would correspond to a fracture (or fault) that is initially critically stressed for shear failure. The fracture with a smaller inclination would be expected to slide more easily, which is also observed in Figs. 20 and 21. As a result, the shear displacement of fractures with smaller inclinations is much bigger than that for those with larger inclination angles (Fig. 22).

4 Concluding Remarks

This paper demonstrates a numerical method which can be used to simulate the nonlinearity and discontinuity of a rock mass. Linking two numerical codes, TOUGH2 and RDCA, this method can track the coupled multiphase fluid flow and geomechanics of rock. One great advantage of the TOUGH–RDCA simulator is its ability to define and model complex, discontinuous geometries independently of the numerical grid, while still being able to model complex multiphase flow and geomechanical processes. In this paper, we presented the development of the simulator and demonstrated its capabilities on synthetic, but practical simulation examples related to critical geomechanical issues, particularly those associated with geologic CO_2 storage in deep sedimentary formations. First, we verified the TOUGH–RDCA against the established TOUGH–FLAC simulator for coupled multiphase flow and geomechanical processes in a reservoir–caprock system without discontinuities. We then tested and demonstrated the TOUGH–RDCA for its ability to capture discontinuities in the caprock, involving single and multiple fractures of various geometries. Finally, we demonstrated how the TOUGH–RDCA can be used to study injection-induced fracture opening, CO_2 migration and potential leakage through the caprock, and injection-induced shear activation of inclined fractures. The TOUGH–RDCA has the potential for modeling fracture propagation through the mesh, with the multiphase flow applications of such a capability to be developed and tested in the near future.

Acknowledgments This work was finically supported by the National Natural Science Foundation of China (Nos. 10972231, 41272349, 11002154) and the National Basic Research Program of China under Grant No. 2010CB732006, and in part, supported by the US Department of Energy under contract No. DE-AC02-05CH11231. We thank Daniel Hawkes at LBNL for reviewing the initial version of the paper.

References

Börgesson L (1996) ABAQUS. Dev Geotech Eng 79:565–570

Bower K, Zyvoloski G (1997) A numerical model for thermo-hydro-mechanical coupling in fractured rock. Int J Rock Mech Min Sci 34(8):1201–1211

Corey AT (1954) The interrelation between gas and oil relative permeabilities. Prod Month 19(1):38–41

Feng XT, Pan PZ et al (2006) Simulation of the rock microfracturing process under uniaxial compression using an elasto-plastic cellular automaton. Int J Rock Mech Min Sci 43(7):1091–1108

Ferronato M, Gambolati G et al (2010) Geomechanical issues of anthropogenic CO_2 sequestration in exploited gas fields. Energy Convers Manage 51(10):1918–1928

Guvanasen V, Chan T (1995) A new three-dimensional finite-element analysis of hysteresis thermohydromechanical deformation of fractured rock mass with dilatance in fractures, Vienna, Austria, pp 347–422

Israelsson JI (1996a) Short description of FLAC version 3.2. Dev Geotech Eng 79:513–522

Israelsson JI (1996b) Short descriptions of UDEC and 3DEC. Dev Geotech Eng 79:523–528

Itasca Consulting Group I (2000) PFC3D user's guide. Itasca Consulting Group Inc., Mineapolis

Kohl T, Hopkirk R (1995) The finite element program "FRACTure" for the simulation of Hot Dry Rock reservoir behavior. Geothermics 24(3):345–359

Neuzil C (2003) Hydromechanical coupling in geologic processes. Hydrogeol J 11(1):41–83

Nguyen T (1996) Description of the computer code FRACON. Dev Geotech Eng 79:539–544

Noorishad J, Tsang C et al (1984) Coupled thermal-hydraulic-mechanical phenomena in saturated fractured porous rocks: numerical approach. J Geophy Res 89(B12):10365

Ohnishi Y, Kobayashi A et al (1996) Coupled thermo-hydro-mechanical processes of fractured media. In: Developments in Geotechnical Engineering, vol 79. Elsevier, pp 545–549

Olivella S, Carrera J et al (1994) Nonisothermal multiphase flow of brine and gas through saline media. Transp Porous Media 15(3):271–293

Pan PZ, Feng XT et al (2009a) Coupled THM processes in EDZ of crystalline rocks using an elasto-plastic cellular automaton. Environ Geol 57(6):1299–1311

Pan PZ, Feng XT et al (2009b) Study of failure and scale effects in rocks under uniaxial compression using 3D cellular automata. Int J Rock Mech Min Sci 46(4):674–685

Pan P-Z, Yan F et al (2012) Modeling the cracking process of rocks from continuity to discontinuity using a cellular automaton. Comput Geosci 42:87–99

Pruess K, Moridis G et al (1999) TOUGH2 user's guide, version 2.0, Lawrence Berkeley National Laboratory Berkeley, CA

Pruess K, Spycher N (2007) ECO2 N-A fluid property module for the TOUGH2 code for studies of CO_2 storage in saline aquifers. Energy Convers Manag 48(6):1761–1767

Rohmer J, Seyedi DM (2010) Coupled large scale hydromechanical modelling for caprock failure risk assessment of CO_2 storage in deep saline aquifers. Oil Gas Sci Technol Revue de l'Institut Français du Pétrole 65(3):503–517

Rutqvist J (2011) Status of the TOUGH-FLAC simulator and recent applications related to coupled fluid flow and crustal deformations. Comput Geosci 37(6):739–750

Rutqvist J (2012) The geomechanics of CO_2 storage in deep sedimentary formations. Geotech Geol Eng 30(3):525–551

Rutqvist J, Stephansson O (2003) The role of hydromechanical coupling in fractured rock engineering. Hydrogeol J 11(1):7–40

Rutqvist J, Tsang CF (2002) A study of caprock hydromechanical changes associated with CO_2-injection into a brine formation. Environ Geol 42(2):296–305

Rutqvist J, Tsang CF (2012) Multiphysics processes in partially saturated fractured rock: experiments and models from Yucca Mountain. Rev Geophys 50(3):RG3006

Rutqvist J, Börgesson L et al (2001) Thermohydromechanics of partially saturated geological media: governing equations and formulation of four finite element models. Int J Rock Mech Min Sci 38(1):105–127

Rutqvist J, Wu YS et al (2002) A modeling approach for analysis of coupled multiphase fluid flow, heat transfer, and deformation in fractured porous rock. Int J Rock Mech Min Sci 39(4):429–442

Rutqvist J, Vasco DW et al (2010) Coupled reservoir-geomechanical analysis of CO_2 injection and ground deformations at In Salah, Algeria. Int J Greenhouse Gas Control 4(2):225–230

Swenson D, DuTeau R et al (1997) A coupled model of fluid flow in jointed rock applied to simulation of a hot dry rock reservoir. Int J Rock Mech Min Sci Geomech Abstr 34:308

Thomas HR, Sansom MR (1995) Fully coupled analysis of heat, moisture, and air transfer in unsaturated soil. J Eng Mech 121:392

Tran D, Nghiem L et al (2010) Study of geomechanical effects in deep aquifer CO_2 storage. In: 44th US Rock Mechanics Symposium and 5th US-Canada Rock Mechanics Symposium, Salt Lake City, Utah, 27–30 June 2010

Tsang CF (1999) Linking thermal, hydrological, and mechanical processes in fractured rocks 1. Annu Rev Earth Planet Sci 27(1):359–384

van Genuchten MT (1980) A closed-form equation for predicting the hydraulic conductivity of unsaturated soils. Soil Sci Soc Am J 44(5):892–898

Wang W, Kolditz O (2007) Object-oriented finite element analysis of thermo-hydro-mechanical (THM) problems in porous media. Int J Numer Meth Eng 69(1):162–201